Physica Scripta. Vol. T69, 98–102, 1997

Photon Induced Resonances in the Current through a Quantum Dot with Zero-Dimensional States

T. H. Oosterkamp, L. P. Kouwenhoven, A. E. A. Koolen, N. C. van der Vaart and C. J. P. M. Harmans

Department of Applied Physics and Delft Institute of Microelectronics and Submicron-technology (DIMES), Delft University of Technology, P.O. Box 5046, 2600 GA Delft, The Netherlands

Received July 19, 1996; accepted August 27, 1996

Abstract

We have measured photon-assisted tunneling through a quantum dot with zero dimensional (0D) states. When the photon energy exceeds the separation between 0D-states we observed photon induced excited state resonances, as well as photon sideband resonances. We study the strength of these resonances as a function of the applied microwave field, and compare them to calculations.

The transport properties of quantum dots at zero frequency have been extensively studied and by now most aspects are well understood. Some studies have been performed where finite but still low frequency signals were applied to a gate electrode nearby the quantum dot. At kHz frequencies Ashoori *et al.* [1] have performed capacitance spectroscopy of quantum dots. At MHz frequencies quantum dots can be operated as turnstiles or pumps [2]. These frequencies f are low in the sense that the photon energy hf is much smaller than the thermal energy k_BT and thus the discrete photon character cannot be discerned. At the high frequency side far-infrared studies in the THz regime have revealed the excitation spectrum of the collective modes [3]. However as described by the generalized Kohn theorem [3], the dipole field of far-infrared radiation does not couple to the relative coordinates of the electrons in a parabolic quantum dot. This means that effects due to electron-electron interactions are not seen in far-infrared transmission experiments. Recent inelastic light scattering experiments have been able to measure electronic excitations in arrays of quantum dots which can be related to a discrete single particle spectrum [4].

We have studied discrete photon effects in the microwave range of 25–75 GHz. At these frequencies $hf \gg k_BT$ at low temperatures. In the absence of microwaves, current can flow through a quantum dot when a discrete energy state is aligned to the Fermi energies of the leads. This current is carried by resonant elastic tunneling of electrons between the leads and the dot. An additional time-varying potential $V\cos(2\pi ft)$ can induce *inelastic* tunnel events when electrons exchange photons of energy hf with the oscillating field. This inelastic tunneling with discrete energy exchange is known as photon-assisted tunneling (PAT). PAT has been studied before in superconductor-insulator-superconductor tunnel junctions [5], in superlattices [6], and in quantum dots [7, 8]. The quantum dots that some of us studied previously [7] were rather large and effectively had a continuous density of states. So far, PAT through small quantum dots with discrete states have only been studied theoretically [9, 10]. In this paper we show different types of PAT processes through a quantum dot with well resolved discrete 0D-states. We show that an elastic resonant tunneling peak in the current develops photon sideband resonances when we apply microwaves. When the photon energy exceeds the separation between 0D-states we also observe photon induced excited states resonances. We study the strength of these resonances as a function of the applied microwave field and compare them to calculations.

Transport through a quantum dot is dominated by Coulomb blockade effects [11]. The energy to add an extra electron to a quantum dot constitutes the charging energy E_c for a single electron, and a finite energy difference $\Delta\varepsilon$ arising from the confinement. A dot is said to have 0D-states if $\Delta\varepsilon$ is larger than the thermal energy k_BT [11]. Assuming sequential tunneling of single electrons, the current can be calculated with a master equation [12]. In Ref. 13 we combine this approach with the Tien-Gordon theory [5] to calculate the effect of microwaves on the d.c. current through a dot with 0D-states. The basic idea is that an a.c. voltage drop $V = \tilde{V}\cos(2\pi ft)$ over a tunnel barrier modifies the tunnel rate [7]:

$$\tilde{\Gamma}(E) = \sum_n J_n^2(\alpha)\Gamma(E + nhf) \tag{1}$$

where $\tilde{\Gamma}(E)$ and $\Gamma(E)$ are the tunnel rates at energy E with and without an a.c. voltage, respectively. $J_n^2(\alpha)$ is the square of the nth order Bessel function evaluated at $\alpha = (e\tilde{V}/hf)$, which gives the probability that tunneling electrons absorb ($n > 0$) or emit ($n < 0$) n photons of energy hf. This equation is valid when the frequency is larger than the tunnelrate, $f \gg \Gamma$. In this model the a.c. electric field is assumed to be confined to the barriers; there are no oscillating electric fields inside the dot or in the leads which could cause transitions within the dot or within the leads.

The diagrams in Fig. 1(a) show two relevant energy states for N electrons in the dot. For small d.c. bias voltage and no a.c. voltages a current resonance occurs when the topmost energy state (i.e. the electrochemical potential) of the quantum dot lines up with the Fermi levels of the leads (see the diagram ε_0). When high frequency voltages drop across the two barriers, additional current peaks appear. These peaks are most clearly distinguishable when the a.c. voltage drop is the same for each barrier. We distinguish two mechanisms which were calculated in Ref. 10. The first mechanism gives photon induced current peaks when the *separation* between the ground state ε_0 and the Fermi levels of the leads *matches* the photon energy (or nhf), as depicted in the diagrams labeled by $\varepsilon_0 + hf$ and $\varepsilon_0 - hf$. The minus and plus signs correspond to being before or beyond the main resonance, respectively. Note that also the case of $\varepsilon_0 - hf$ involves photon absorption. Following the literature

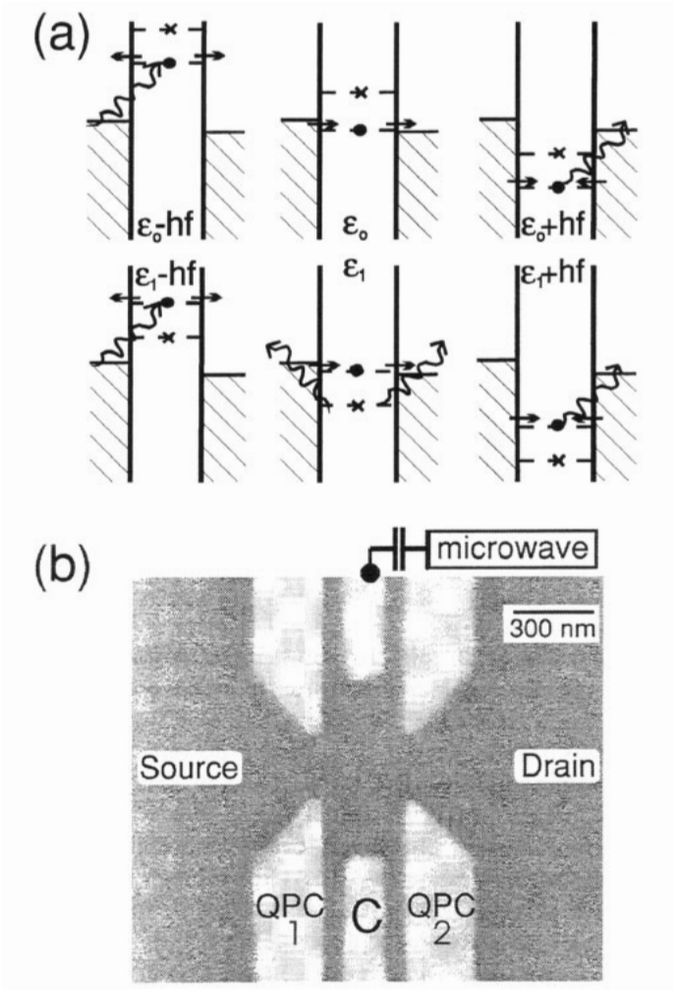

Fig. 1. (a) Diagrams depicting the sequence of tunneling events which dominantly contribute to the current through a quantum dot, for different gate voltages. A small d.c. bias raises the left Fermi level with respect to the right Fermi level. ε_0 and ε_1 denote the groundstate and the first excited state of the N electron system. When the N^{th} electron tunnels to one of the two reservoirs, the energy states of the dot drop by the charging energy E_c. The corresponding diagrams for $N-1$ electrons are not shown. Note that only processes with tunneling from or to states close to the Fermi levels in the leads contribute to the net current. (b) SEM photo of the sample. The lithographic size of the dot is $(600 \times 300)\,\mathrm{nm}^2$. Current can flow when we apply a voltage between source and drain. The microwave signal is coupled to one of the center gates.

on the tunneling time we call these current peaks: sidebands [14]. The second mechanism leads to photon peaks when an excited state is in resonance with the Fermi levels of the leads (see diagram ε_1). Without PAT, transport through the excited state ε_1 is blocked since Coulomb blockade prevents having electrons in both the ground state and the excited state simultaneously. The electron in the ground state cannot escape from the dot because its energy is lower than the Fermi levels in the leads. PAT, however, empties the ground state ε_0 when the electron in ε_0 absorbs enough energy and leaves the dot. This process is analogous to photoionization. Now, the Nth electron can tunnel resonantly via the excited state ε_1 as long as the state ε_0 stays empty [15]. The groundstate may be filled through tunneling from the leads or through relaxation from the excited state to the ground state. The height of the resonance ε_1 will therefore strongly depend on the ratio of the tunnelrates from the leads to the groundstate and the excited state as well as on the relaxation rate from ε_1 to ε_0. More photon peaks are generated when these two mechanisms are combined as in the diagrams labeled by $\varepsilon_1 + hf$ and $\varepsilon_1 - hf$. We thus see that PAT can populate the excited states with the help of tunneling between dot and leads and that PAT is responsible for a number of new current resonances.

It is important to note that in these diagrams only processes with tunneling from or to states close to the Fermi levels in the leads contribute to the net current. Tunnel processes that start with an electron from further below the Fermi level in one of the leads are cancelled by an electron from the other lead. This is only true when the a.c. voltage drop is the same for each barrier. When the a.c. voltage drops across the two barriers are unequal the dot acts as an electron pump [7, 10]. The resulting pumped current makes the current resonances discussed above less clear. For this reason we discuss this pumping mechanism in more detail here before proceeding further. Figure 2 shows a calculation of the pumped current as a function of the gate voltage that occurs when the a.c. voltage drop over one barrier is 5% smaller than over the other barrier. We have taken zero d.c. bias voltage. To illustrate the origin of the pumped current the insets show the extreme case, when all the a.c. voltage drop is across the left barrier. In this case photon absorption occurs only at the left barrier. At negative gate voltage when the ground state level of the dot is *above* the Fermi level of the leads an electron can *enter* the dot from the left lead only (bottom left inset of Fig. 2). Once the electron is in the dot it can tunnel out through both of the tunnelbarriers. Only the electron tunneling out to the right lead contributes to the net current. Therefore the net current is to the right. When the ground state level of the dot is *below* the Fermi level of the leads, however, an electron can only *leave* the dot to the left lead (upper right inset of Fig. 2). The dot can be filled from either lead once it is emptied. This time only the electron tunneling *in* from the right lead contributes to the net current. Therefore there is a net current to the left. The difference between these two situations is the shift in the ground state energy with respect to the Fermi levels of the leads. So, when the gate voltage is swept such that the ground state moves through the Fermi levels of the leads, the pumped current changes sign. The pumped current occurs over a width which scales with the photon energy.

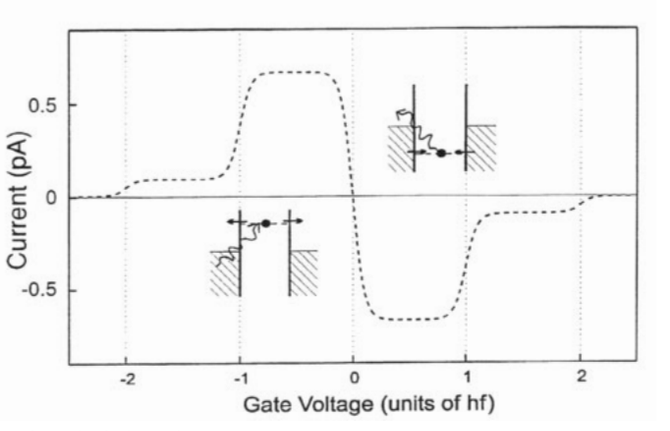

Fig. 2. Calculation of the current as a function of gate voltage in the case where the a.c. voltage drop over one barrier is 5% smaller than over the other barrier. $V = 0$, $k_B T = 0.05hf$, $\Gamma = 5 \cdot 10^8\,\mathrm{s}^{-1}$. The insets depict which sequence of tunneling events is responsible for the pumped current when the ground state of the quantum dot is below or above the Fermi levels of the leads.

The extra shoulders at the far left and far right of the figure are due to two-photon processes.

Our measurements are performed on a quantum dot defined by metallic gates [see Fig. 1(b)] in a GaAs/AlGaAs heterostructure containing a 2 dimensional electron gas (2DEG) 100 nm below the surface. The 2DEG has mobility $2.3 \cdot 10^6\,\mathrm{cm^2/Vs}$ and electron density $1.9 \cdot 10^{15}\,\mathrm{m^{-2}}$ at 4.2 K. By applying negative voltages to the two outer pairs of gates, we form two quantum point contacts (QPCs). An additional pair of center gates between the QPCs confines the electron gas to a small dot. No electron transport is possible through the narrow channels between the center gates and the gates forming the QPCs. The center gate voltage V_g can shift the states in the dot with respect to the Fermi levels of the leads and thereby controls the number of electrons in the dot. The energy shift is given by $\Delta E = \kappa \cdot \Delta V_g$. A small d.c. voltage bias is applied between source and drain and the resulting d.c. source-drain current is measured. From standard d.c. measurements we find that the effective electron temperature is approximately $T = 200\,\mathrm{mK}$ and the charging energy $E_c = 1.2 \pm 0.1\,\mathrm{meV}$. We independently determine the level splitting $\Delta\varepsilon$ for different magnetic fields from current-voltage characteristics. In addition to the d.c. gate voltages we couple a microwave signal (10–75 GHz) capacitatively into one of the center gates. The microwave signal will not couple in the same way to the dot as to the leads, which results in an a.c. voltage drop over the barriers.

In the following we first present some experimental results with a strongly pumped current. Then we discuss the measurements on the photon resonances. Figure 3 shows measurements of the current at $B = 1.96\,\mathrm{T}$ for three frequencies around 47.4 GHz (the arrow denotes hf). The dashed line is the current without microwaves. All curves are taken with a bias voltage of $V = 13\,\mu\mathrm{V}$. It can be seen that for the lowest frequency the current is pumped in one direction whereas for the highest frequency it is pumped in the opposite direction, meaning that while at 47.33 GHz the left barrier has the *smaller* a.c. voltage drop, at 47.43 GHz the left barrier has the *larger* a.c. voltage drop. This illustrates how sensitively the asymmetry of the voltage drops over the two barriers depends on the frequency. This sensitivity is ascribed to the standing waves in the sample holder. The dotted line shows the current measured at an intermediate frequency, where we expect the a.c. voltage drop to be equal over both barriers. In contrast to the two solid curves, the dotted line is lower than the dashed line without microwaves over the whole gate voltage range. This cannot be explained by the pumping mechanism in our model. Our model only includes the oscillation of the potential of the leads and the dots which always results in a pumped current which changes sign at the resonance. This pumped current which is negative over the whole gate voltage range is attributed to the effect of the microwaves on the barrier height. The inset shows how a quantum dot can act as a pump when one tunnelbarrier is periodically modulated in height. During one part of the cycle when the left barrier is low electrons enter the dot ($\Gamma_L^{low} > \Gamma_R$) while they escape the dot through the right barrier in the second half of the cycle when the left barrier is high ($\Gamma_L^{high} < \Gamma_R$). This essentially is a classical mechanism that has been verified experimentally in the MHz regime.

For observing photon resonances we choose frequencies that do not lead to a d.c. current in the absence of a d.c. bias voltage, in order to minimize both types of pumping. It is then easier to distinguish the photon resonances. Figure 4 shows measurements of the current at $B = 0.91\,\mathrm{T}$ [16] and for $f = 61.5\,\mathrm{GHz}$. As we increase the power we see extra peaks coming up. We label the peaks as in Fig. 1(a). On the right side of the main resonance a new resonance appears, which we assign to photoionization followed by tunneling through the first excited state. At higher powers the one-photon sidebands of the main resonance as well as those of the excited state resonance appear. We do not observe the expected peak for $\varepsilon_0 + hf$ in this measurement. The arrows underneath the curves mark the photon energy $hf = 254\,\mu\mathrm{eV}$. Elsewhere [17] we identify the peaks by looking at the linear frequency scaling of the peak position. The peaks ε_0 and ε_1 remain in place when we change the frequency, since the photon energy evidently does not alter the energy splitting. The other peaks, $\varepsilon_0 - hf$ and $\varepsilon_1 \pm hf$, shift by an amount which corresponds to the change in photon energy. This reflects the fact that the sidebands originate from matching the states ε_0 and ε_1 to the Fermi levels of the leads by a photon energy hf.

Now that the pumping is less strong we can study the resonances in more detail. Figure 5(a) shows a calculation of

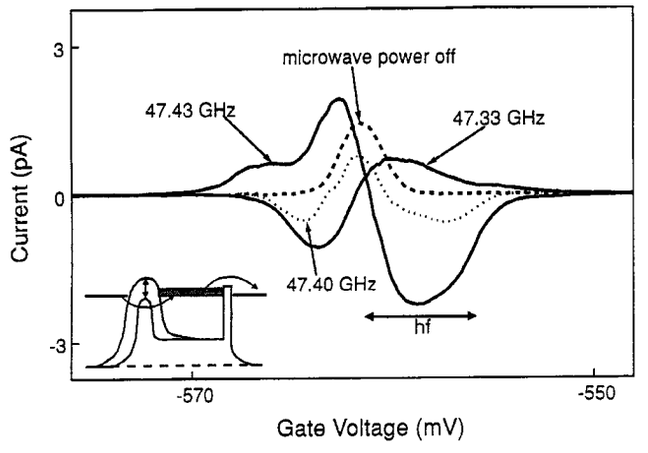

Fig. 3. Measurements of the pumped current at $B = 1.96\,\mathrm{T}$, $V = 13\,\mu\mathrm{V}$ and for frequencies around 47.4 GHz. Dashed line is without microwaves. The dotted line shows the smallest asymmetry, but shows evidence for a pumping mechanism which is not included in our model.

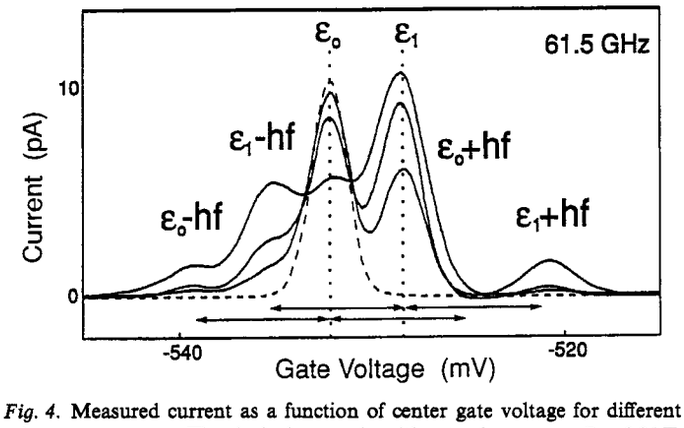

Fig. 4. Measured current as a function of center gate voltage for different microwave powers. The dashed curve is without microwaves. $B = 0.91\,\mathrm{T}$, $V = 13\,\mu\mathrm{V}$, $f = 61.5\,\mathrm{GHz}$. The main resonance ε_0 and the resonance attributed to the excited state ε_1 are clearly observed. The other peaks, $\varepsilon_0 - hf$ and $\varepsilon_1 \pm hf$ are separated from ε_0 and ε_1 by a photon energy as indicated by the arrows. We do not observe $\varepsilon_0 + hf$ in this measurement.

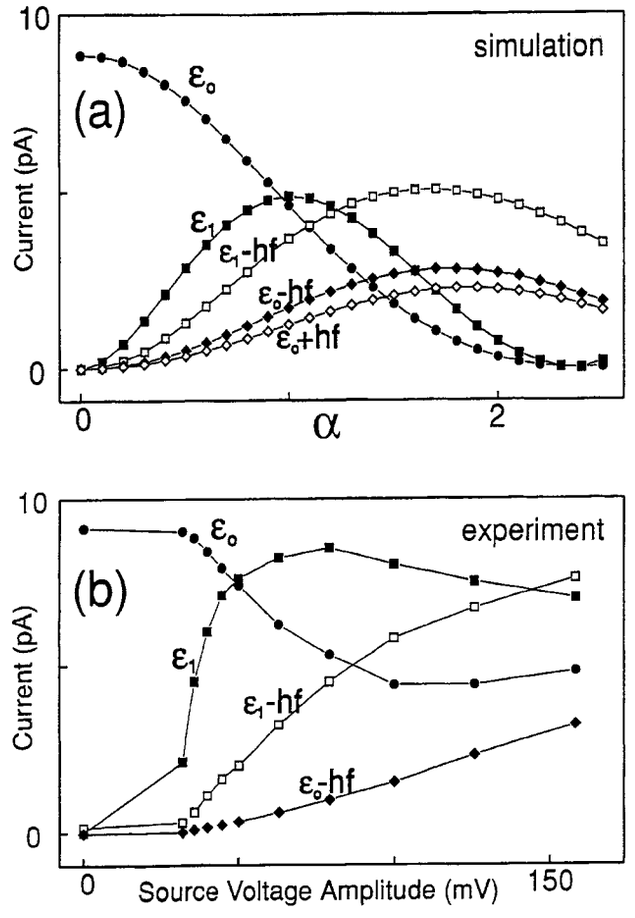

Fig. 5. (a) calculation of the peakheights as a function of the a.c. voltage drop across the barriers $\alpha = (e\tilde{V}/hf)$. $T = 200\,\text{mK}$, $V = 13\,\mu\text{V}$, $f = 52.5\,\text{GHz}$. The tunnelrates from the leads to the groundstate and the excited state are set to $\Gamma_{\varepsilon_0} = 5 \cdot 10^8\,\text{s}^{-1}$ and $\Gamma_{\varepsilon_1} = 14 \cdot 10^8\,\text{s}^{-1}$, respectively. The relaxation rate from the excited state to the ground state is assumed to be zero in the calculation. (b) experimentally obtained peakheights as a function of the a.c. voltage source voltage amplitude. $V = 13\,\mu\text{V}$, $f = 52.5\,\text{GHz}$. The tunnelrates, obtained from d.c. current-voltage characteristics, are $\Gamma_{\varepsilon_0} = 5 \cdot 10^8\,\text{s}^{-1}$ and $\Gamma_{\varepsilon_1} = 6 \cdot 10^8\,\text{s}^{-1}$.

the peak heights as a function of the a.c. voltage drop across the barriers $\alpha = (e\tilde{V}/hf)$. These results were obtained using the master equation approach described in Ref. 13. Temperature, bias voltage and frequency are taken from the experiment described below: $T = 200\,\text{mK}$, $V = 13\,\mu\text{V}$ and $f = 52.5\,\text{GHz}$. The tunnelrates from the leads to the groundstate and the excited state are set to $\Gamma_{\varepsilon_0} = 5 \cdot 10^8\,\text{s}^{-1}$ and $\Gamma_{\varepsilon_1} = 14 \cdot 10^8\,\text{s}^{-1}$, respectively. The relaxation rate from the excited state to the ground state is assumed to be zero in the calculation. The effect of a finite relaxation rate is to reduce the height of ε_1 with respect to the other peaks since it would make the process ε_1 described above less effective. The calculated peak heights roughly follow the Bessel functions in eq. 1. The groundstate resonance ε_0 follows $J_0^2(\alpha)$ since it involves only elastic tunnelevents (see Fig. 1(a), diagram ε_0). The photon sidebands follow $J_1^2(\alpha)$, since they solely depend on the probability of photon absorption. For example the process $\varepsilon_0 - hf$ is due to a photon assisted tunnel event which fills the dot. Once the dot is filled, however, it does not matter whether the dot is emptied via an elastic or an inelastic event. The process ε_1 follows the product of the first and second order Bessel functions $J_0^2(\alpha)J_1^2(\alpha)$ since it requires that the ground state is emptied via a PAT process but also that the following tunneling processes through the excited state ε_1 are elastic. Figure 5(b) shows the experimental results for the peak heights are $B = 0.91\,\text{T}$ and $f = 52.5\,\text{GHz}$ as a function of the a.c. voltage amplitude at the output of the source. The measurements are in good qualitative agreement below an a.c. source voltage of 100 mV. At higher a.c. voltages the pumped current starts to become important. The values for the tunnelrates to ε_0 and to ε_1 derived from the d.c. current-voltage characteristic are $\Gamma_{\varepsilon_0} = 5 \cdot 10^8\,\text{s}^{-1}$ and $\Gamma_{\varepsilon_1} = 6 \cdot 10^8\,\text{s}^{-1}$. The value for Γ_{ε_1} in the calculation is larger than the experimentally determined value but still the calculated value for the height of the ε_1 resonance is smaller than the experimental value. It is a general trend in most of our data that the peak ε_1 is higher than predicted by our model and that $\varepsilon_0 + hf$ is lower than expected from simulations. At present this is not understood. Future calculations would have to investigate these deviations from the Tien–Gordon theory.

Simulations show that the pumped current is quite independent of the bias voltage when $eV \ll hf$ while current due to the photon resonances increases linearly with the bias voltage when $eV < k_B T$. Therefore it is possible to improve the quality of our data by separating the pumped current from the photon resonances. This can be done by doing measurements for different bias voltages at every microwave power. This would allow for better comparison with calculations over a wider range of microwave powers.

In conclusion, we have used photon-assisted tunneling to study the interaction between microwave fields and electrons occupying discrete 0D-states in a single quantum dot. Our experimental results may provide a way to measure deviations from Tien–Gordon theory and to determine the relaxation rates of a quantum dot. They also show the feasibility of recently proposed experiments on Rabi-type oscillations between coupled quantum dots [18, 19].

Acknowledgements

We thank S. F. Godijn, K. Ishibashi, J. E. Mooij, Yu. V. Nazarov and T. H. Stoof for discussions and experimental help. We thank Philips Laboratories and C. T. Foxon for providing the heterostructures. The work was supported by the Dutch Foundation for Fundamental Research on Matter (FOM). L.P.K. was supported by the Royal Netherlands Academy of Arts and Sciences (KNAW).

References

1. Ashoori, R. C. *et al.*, Phys. Rev. Lett. **71**, 613 (1993).
2. Kouwenhoven, L. P. *et al.*, Zeitschrift für Physik **85**, 381 (1991).
3. Merkt, U., Physica B **189**, 165 (1993) and references therein.
4. Strenz, R. *et al.*, Phys. Rev. Lett. **73**, 3022 (1994) and references therein.
5. Tien, P. K. and Gordon, J. R., Phys. Rev. **129**, 647 (1963).
6. Guimares, P. S. S. *et al.*, Phys. Rev. Lett. **70**, 3792 (1993); Keay, B. J. *et al.*, Phys. Rev. Lett. **75**, 4098 (1995); Keay, B. J. *et al.*, Phys. Rev. Lett. **75**, 4102 (1995).
7. Kouwenhoven, L. P. *et al.*, Phys. Rev. B **50**, 2019 (1994) and Phys. Rev. Lett. **73**, 3433 (1994).
8. Blick, R. H. *et al.*, Appl. Phys. Lett. **67**, 3924 (1995).
9. Sokolovski, D. Phys. Rev. B **37**, 4201 (1988).
10. Bruder, C. and Schöller, H., Phys. Rev. Lett. **72**, 1076 (1994).
11. See for reviews on quantum dots: Meirav, U. and Foxman, E. B., Semiconductor Science and Technology **10**, 255 (1995); Kouwenhoven, L. P. and McEuen, P. L., to be published in: "Nano-Science and Technology", G. Timp ed. (AIP Press, New York).

12. Averin, D. V., Korotkov, A. N. and Likharev, K. K., Phys. Rev. B **43**, 6199 (1991); Beenakker, C. W. J., Phys. Rev. B **44**, 1646 (1991).
13. Oosterkamp, T. H. *et al.*, Semiconductor Science and Technology, to be published.
14. Büttiker, M. and Landauer, R., Phys. Rev. Lett. **49**, 1739 (1982).
15. Note that for this second mechanism *nhf* has to *exceed*, but not necessarily *match* the energy splitting $\Delta\varepsilon = \varepsilon_1 - \varepsilon_0$.
16. PAT is also observed at $B = 0$ but with less resolution due to a higher effective electron temperature at $B = 0$.
17. Oosterkamp, T. H. *et al.*, Phys. Rev. Lett., submitted to.
18. Stoof, T. H. and Nazarov, Yu. V., Phys. Rev. B **53**, 1050 (1996); Stafford, C. A. and Wingreen, N. S., Phys. Rev. Lett. **76**, 1916 (1996).
19. Fujisawa, T. and Tarucha, S., Superlattices and Microstructures, to be published.